Integrity of Metallic Medical Implants in Physiological Solutions

F. El-Taib Heakal[1,], O.S. Shehata[2], N.S. Tantawy[3]*

[1] Chemistry Department, Faculty of Science, Cairo University, Giza 12613, Egypt.
[2] Physical Chemistry Department, National Research Centre, Dokki, Giza, Egypt.
[3] Faculty of Girls for Arts, Science and Education, Ain Shams University, Asma Fahmi Street, Cairo, Egypt.
[*]E-mail: feltaibheakal@gmail.com

Stainless steel and Ti alloys are increasingly used as biomaterials for implants and prosthesis because of their lower elasticity modulus and superior biocompatibility. In the present study different electrochemical measurements have been used to characterize the *in vitro* surface integrity of two surgical grade alloys: 316L stainless steel (SS) and Ti-6Al-4V alloy (TA). Both alloys are commonly used for orthopaedic and ostesynthesis implants. The aim was to compare their corrosion performance during soaking over an extended period of time in two physiological solutions; Ringer saline (RS) and phosphate buffer saline (PBS). The open circuit potential indicated that both samples exhibit spontaneous passivation. Electrochemical impedance spectroscopy (EIS) data revealed that the corrosion mechanism of both alloys can be modified according to the chemical composition of the test solution. Hence, RS was found to be more corrosive than PBS, especially for SS which possesses higher corrosion rate than TA. However, in PBS the passive traits of SS become comparable to those for TA due to PO_4^{3-} contamination, as confirmed by SEM and EDX examinations.

1. INTRODUCTION

The need for metallic materials in medical applications continuously increases as implants to restore lost functions or replace organs functioning below acceptable levels [1]. This is because metals are more suitable for load-bearing applications compared with ceramics or polymeric materials, mainly due to their combined high mechanical strength and fracture toughness [2,3]. Nevertheless, corrosion of metallic implants is one of the most critical issues in their use because it could affect negatively their biocompatibility and mechanical integrity. The *in vivo* implants encounter different physical and chemical environments and their interaction with the tissues and bones is a complex problem [1]. The

first and foremost point for the choice of the biomaterial is its acceptability by the human body. Oxide layer on the metallic implant surface can facilitate the rapid fixation of viable bone to the metal without soft-tissue layer [4]. However, the improve in this process depends on the surface characteristics of the implant such as surface morphology, roughness and chemical composition to promote bone apposition [5,6].

Among the typically approved metallic biomaterials, stainless steel, cobalt-chromium and titanium-based alloys are the most widely used implants for orthopaedic applications in clinical practice [3,7]. This is because they are highly resistant to different forms of corrosion with each material having its own advantage. Nevertheless, the introduction of metal alloys into human body is not completely innocuous, since for example they may interact with the aggressive environment containing chloride ions. This will lead to release of toxic and potentially carcinogenic metallic species [8,9]. Large concentration of prosthesis derived cations can disturb cell behavior, and may eventually lead to implant failure and severe complications [8]. Metal release from the orthopaedic implants into surrounding tissue occurs by various mechanisms, including corrosion, wear and mechanically accelerated electrochemical processes such as stress corrosion, corrosion fatigue, fretting corrosion and tribocorrosion [10]. This metal release has been associated with clinical implant failure, osteolysis, cutaneous allergic reactions and remote site accumulation [11]. In this respect, Okazaki and Gotoh [12] found that the quantity of Ti released from both Ti-6Al-4V and Ti-6Al-7Nb alloys increased with decreasing pH (pH ≤ 4) , and markedly attenuated at pHs of ~4 and higher. In all solutions, the amount of Ti released from the latter alloy was always smaller than that released from the former one. Likewise, the quantity of Al released from the two Ti materials gradually decreased with increasing pH. The same authors indicated also that the quantity of Fe and Ni released from stainless steel gradually decreased with the increase in the environment pH. On the other hand, the difference in the quantity of Co released from Co-Cr-Mo alloy was relatively small in all solutions, and the quantities of Cr and Mo released from stainless steel or the Co-Cr-Mo alloy were found to be smaller at pH ≥ 4 [12].

Due to formation of surface passive layers consisting mainly from amorphous titanium dioxide [13,14], which is thermodynamically stable over a wide range of potential and pH [15], titanium alloys have been widely used as dental and implant materials. Sometimes, a small amount of suboxides TiO, Ti_2O_3 was found to be present closer to the inner metal/oxide film interface [16,17], otherwise the potential gradient would be large. In general, titanium alloys can be divided into single α (and near-α) alloys and two-phase α-β alloys, as well as the more recent developed metastable β alloys [18]. The introduction of the β-phase increases the strength of the alloy which is important for aerospace and biomedical applications. The Ti-6Al-4V alloy with α-β structure is the first titanium alloy used as implant material, particularly for orthopaedic and osteosynthesis applications [19]. It is generally considered as a standard material when evaluating the fatigue resistance of a new orthopaedic titanium alloy [18]. On the other hand, stainless steel is mainly used when stiffness is required, and the grade utilized in implantation is the austenitic AISI 316L [20-22]. This is because it is not ferromagnetic which permits the implanted patients to be examined by using magnetic resonance imaging [23]. The contact between the metallic implant and the host tissues is made through a thin oxide passivating layers formed spontaneously on the implant surface, which allows the osseointegration process [3].

The integrity of the surface oxide film has been strongly correlated with the chemical and mechanical stability of implants [3,22].

The present investigation was aimed to evaluate the corrosion stability of two biometallic materials, the surgical stainless steel (type AISI 316L) and an α-β titanium alloy (Ti-6Al-4V). Among the reasons for choosing these materials are their ability to develop naturally formed passive film which can act as a barrier to metal ion diffusion [24,25]. In addition are their functional and economical aspects compared to cp-Ti or Co-Cr-Mo alloys, being as well spontaneously passivated materials. Although many research works on these two chosen biomedical alloys have been reported in the literature, further work is still needed to compare their behavior in artificial solutions of different compositions. For this scenario, two physiological environments with different nature: Ringer saline (RS) and phosphate buffer saline (PBS) were used as electrolytes to assess the electrochemical performance of the two tested alloys relative to each other. This was made by recording the corrosion resistance with time using electrochemical impedance spectroscopy (EIS) tests, as well as measuring the corrosion kinetic parameters using potentiodynamic polarization scans. SEM and EDX examinations were also used to correlate the electrochemical behavior with the alloy surface microstructure and composition.

2. EXPERIMENTAL

Materials used in this study were an AISI 316L type stainless steel (SS) with composition in wt.% of: 25.5 Cr, 7.6 Ni, 6.1 Mn, 0.5 Mo, 0.02 C and balance Fe; and Ti-6Al-4V titanium alloy (TA) supplied from Johnson and Matthey (England) with composition in wt.% of: 5.7 Al, 3.85 V, 0.18 Fe, 0.038 C, 0.106 O and 0.035 N and balance Ti. The electrodes were in the form of massive cylindrical rods. Each rod (2 cm length and 0.6 cm diameter) was welded to an electrical wire and fixed with Araldite epoxy resin in a glass tube leaving the cross-sectional area of the specimen to face the solution. This type of electrode preparation gave always a fixed exposed surface area of 0.282 cm^2 for both tested materials. Prior to each experiment the working electrode was mechanically ground with finer grades of emery papers (600-1200 grit), degreased with acetone and rinsed with deionized water. Measurements were conducted in two physiological solutions, namely, Ringer saline (RS) containing NaCl, 8.61 g/L; KCl, 0.30 g/L; and CaCl$_2$, 0.49 g/L, pH 7.2 [14, 26,27] and phosphate-buffer saline (PBS) produced by Nissui pharmaceutical co. Ltd., Japan, containing NaCl, 8.0 g/L; KCl, 0.2 g/L; Na$_2$HPO$_4$, 1.42 g/L; and KH$_2$PO$_4$, 0.24 g/L, pH 7.2 [28].

The present study was mainly intended to compare the behavior of the tested samples over a prolonged period of time to detect differences due to sample or solution nature under lab conditions, where the average temperature was close to the human body level. Electrochemical measurements were recorded using a conventional three-electrode Pyrex glass cell furnished with a large platinum sheet (2.0 cm × 4.0 cm × 0.2 cm) and a saturated calomel electrode (SCE), served as counter and reference electrodes, respectively. The tip of the Luggin capillary included in the design was made very close to the surface of the working electrode to minimize the IR drop. All potentials were measured and referred to the SCE reference electrode (E_{SCE} = 0.241 V vs. SHE). EIS studies were

carried out at the open circuit potential (OCP) using the electrochemical workstation IM6e Zahner-elektrik GmbH, Meβtechnik, (Germany) provided with Thales® software. An excitation ac signal of 10 mV peak to peak was used for six frequency decades from 100 kHz to 0.1 Hz, being the measuring frequency limits of the used instrument [24,25]. Bode plots and Nyquist plots were obtained after the specimens were soaked in a naturally aerated test solution for different durations extended up to 14 days. After this time period, potentiodynamic scans were recorded at a rate of 1 mV s^{-1} for each specimen in the respective physiological medium, starting from -1.0 V to +1.0 V vs. SCE. The corrosion current density (j_{corr}) which is equivalent to the corrosion rate was estimated using the extrapolation method, as per as described elsewhere [29,30]. This was done through extrapolating the linear portion of the cathodic polarization curve to meet the vertical line drawn at the potential of zero current in the potentiodynamic curves, i.e. at E_{corr} . This methodology was consistently adopted because the two tested alloys exhibited stable passive behavior, and therefore well-defined Tafel slopes were not observed in the anodic portion of the Tafel polarization curve. In order to verify the reproducibility of all measurements for both samples, each EIS test was repeated three times on a new polished surface with a new portion of solution [14]. The obtained results were found to be reproducible by a percentage of more than 95%.

For SEM and EDX studies, the substrates were soaked in each solution for 11days, then removed, washed with acetone and dried on a clean bench. The surface morphology and composition of each sample after immersion were carried out using the JEOL JXA-840A electron probe micro analyzer (Japan) equipped with energy-dispersive X-ray (EDX) facilities, and employing accelerating voltage of 30 kV.

3. REULTS AND DISCUSSION

3.1. Open circuit potential analyses

The evolution with time for the OCP (E_{oc}) over 14 days immersion period in the two tested solutions are shown in Fig.1 for both samples, as recorded with an accuracy of ± 5 mV. In general, the profile of all transients has nearly similar features in RS and PBS solutions. In any case, the initial E_{oc} value shifts continuously towards the positive direction of potential first with a faster rate and then slowly until it reaches an almost quasi-stationary state. This mode of variation in the OCP indicates similar tendency for the two alloys to grow a spontaneous oxide film, which passivates the metallic surface when in contact with an aerated physiological environment. As claimed by Gurappa [31], the attainment of a steady potential indicates that the passive film remains intact and protective. It is noticed that in RS solution E_{oc} for TA begins initially at more negative potential of -0.23 V(SCE) compared to the value of -0.14 V(SCE) for SS. This implies that SS possesses thicker native oxide film relative to that for TA, thus for SS in RS the metal ions have initially to penetrate an oxide film corresponding to high anodic polarization with respect to the case of TA. However, after the end of the second day E_{oc} for TA becomes more positive with time onwards compared to its value for SS material.
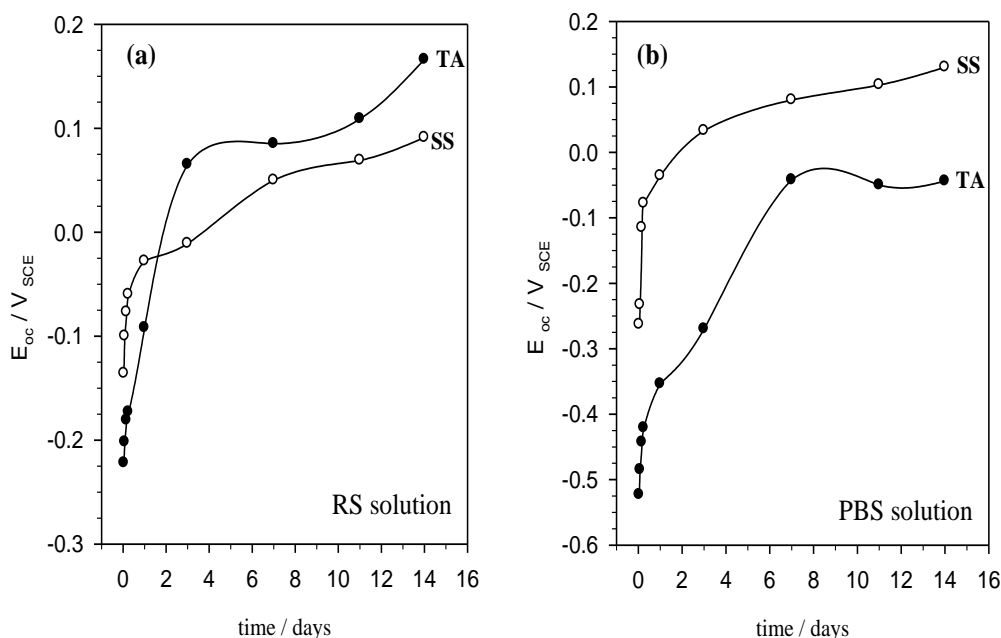
Figure 1. Evolution of the OCP (E_{oc} / V_{SCE}) for both 316L stainless steel (SS) and Ti-6Al-4V alloy (TA) in (a) Ringer saline (RS) and (b) phosphate buffer saline (PBS) solutions.

This is likely attributed to the fast deposition of a more protective oxide film on TA which seals its surface. On the other hand, in PBS solution E_{oc} for SS exhibits always higher potential values than those for TA sample. The results reveal also that for TA sample, E_{oc} at any time interval has more positive value in RS than in PBS solution. This behavior indicates that the oxide film grown on TA surface in RS fluid is probably thicker than the other one grown in PBS [25]. While for SS sample E_{oc} starts at higher value in RS than in PBS solution, and after the first day of electrode immersion the measured potential in PBS medium exceeds its value in the RS and becomes more positive with extending the time.

It is well established that, the increase in an electrode potential is indicative of film healing and thickening [24,32]. But shifting the potential to more positive or more negative values cannot serve as a dependable criterion of decreasing or increasing the corrosion rate. This is because thickness alone is not assumed to provide a criterion of protection, as the kinetics of attack is related to a variety of other factors such as surface film composition, microstructure, continuity and adhesion to the substrate [33,34]. The nature of the formed film being protective or non-protective will be further clarified based on the data of ac and dc techniques.

3.2. Electrochemical impedance analyses

Electrochemical impedance spectroscopy (EIS) is one of the most useful and informative tools for metal corrosion characterization and assessment, therefore, it can be able to provide reliable data for determination of the passive film structure [19,24,25,31].
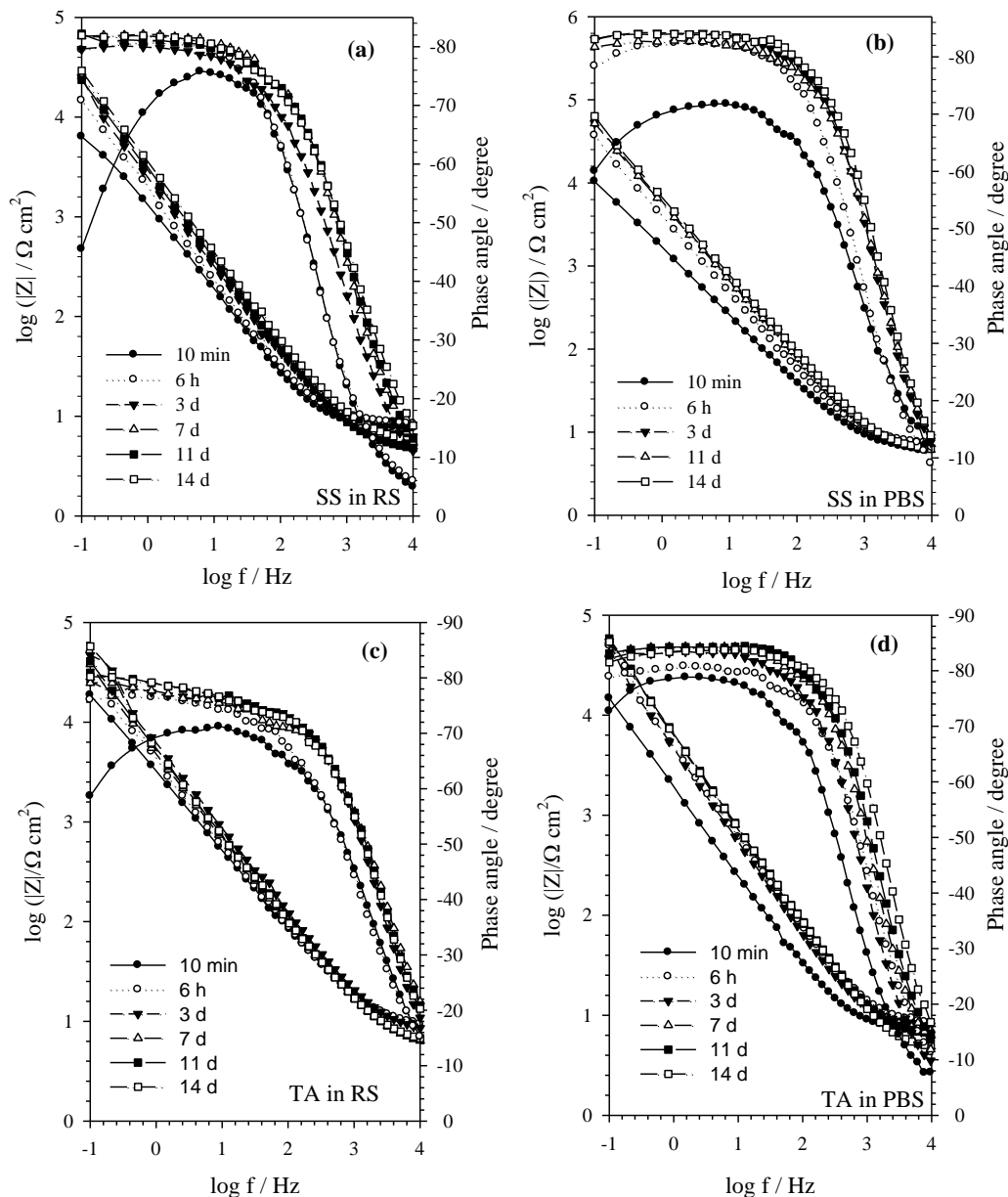
Figure 2. The Bode plots for: (a,b) 316L stainless steel (SS) and (c,d) Ti-6Al-4V alloy (TA) as a function of time in Ringer saline (RS) and phosphate buffer saline (PBS) solutions, respectively.

Impedance spectra for both SS and TA samples at different immersion times extended up to 14 days are shown in Figs. 2 and 3 as Bode and Nyquist plots, respectively. Generally, the spectra on each format exhibit similar behavior for the different durations in the two tested environments. This similarity implies that the corrosion mechanisms for those systems are the same, albeit with different corrosion rates depending on the solution chemistry [19,25]. The Bode plots of the two samples shown in Fig. 2 reveal that, although the impedance spectra are measured down to very low frequency values, no resistive region (horizontal line associated with phase angle $\theta \sim 0^{o}$) can be discerned over this frequency range [25,30]. The responses are in good agreement with the previously obtained spectra by other authors [13,19]. This indicates highly capacitive behavior, typical of passive materials from

medium to low frequencies by phase angles approaching −90°, and suggesting that a highly stable protecting film is formed on the alloy surfaces under all conditions. On the other hand, over the high frequency region the impedance modulus (|Z|) of each alloy tends to become frequency independent with a phase angle falling rapidly towards zero as *f* increases, revealing generally resistive behavior due to the solution resistance between the working and reference electrode [30,35]. Moreover, at the low frequency region the peak of the phase angle Bode plot becomes broader and the absolute impedance curve increases continuously with increasing immersion time until the end of the eleventh day then decreases afterward. The reduction in the impedance value observed after 11 days immersion indicating accordingly a decrease in the stability and corrosion resistance of the material.
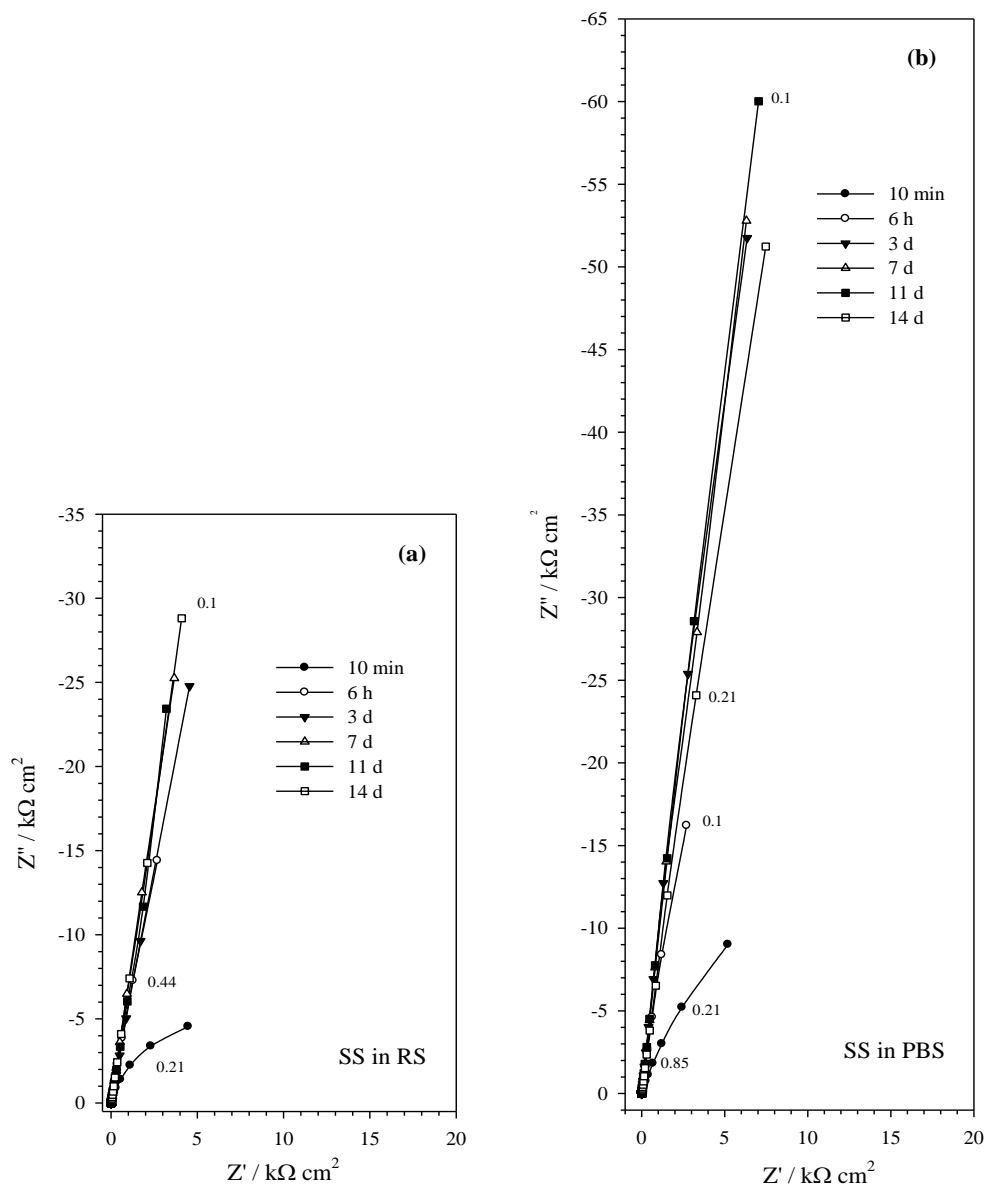
Figure 3(a,b). The Nyquist plots for 316L stainless steel (SS) as a function of time in Ringer saline (RS) and phosphate buffer saline (PBS) solutions, respectively.
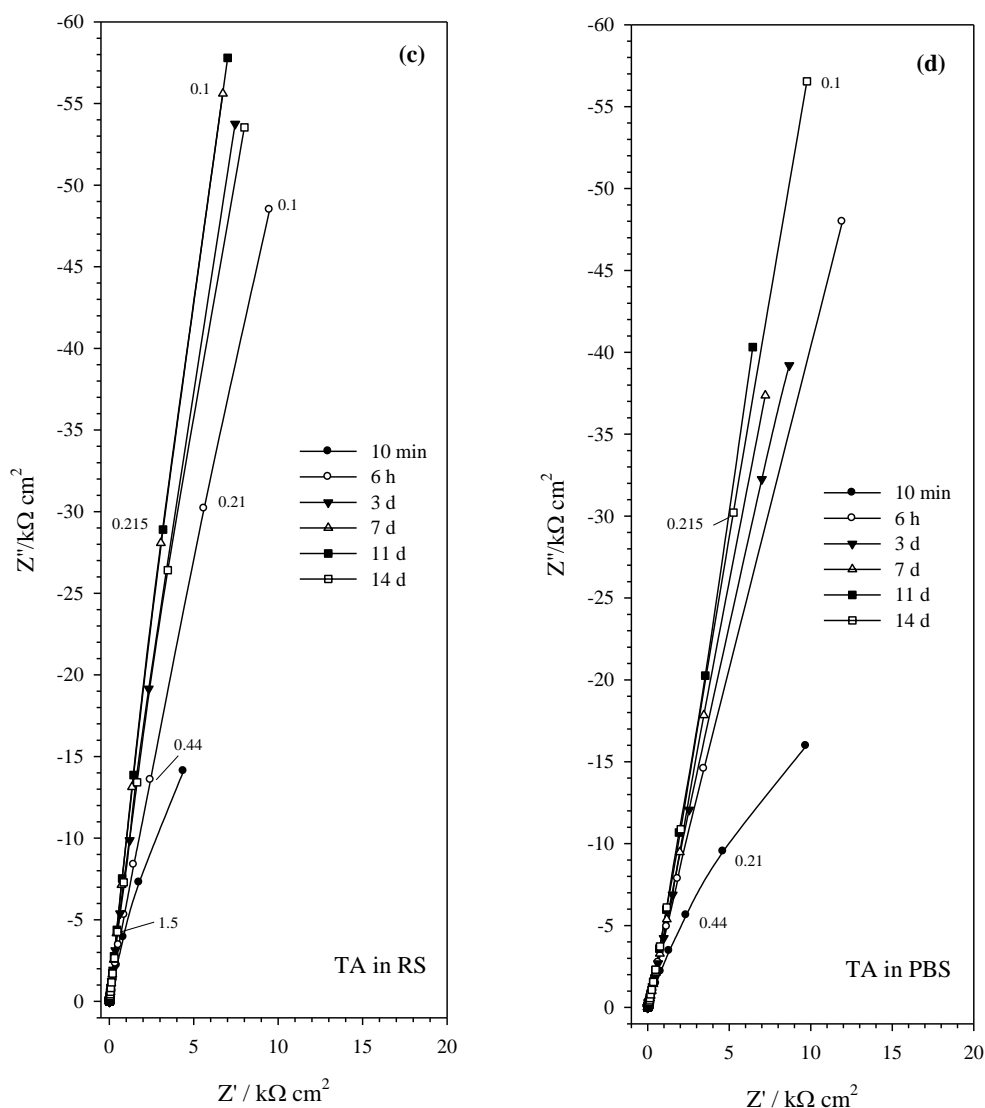
Figure 3(c,d). The Nyquist plots for Ti-6Al-4V (TA) as a function of time in Ringer saline (RS) and phosphate buffer saline (PBS) solutions, respectively.

In fact, the behavior of the impedance responses as represented on the Bode format (Fig. 2) corroborates well with their trends on the Nyquist format depicted in Fig. 3. For both samples, a careful inspection of the obtained complex plane diagrams reveals that they are all no longer ideal capacitive semicircles, but arcs of semicircles with centers depressed below the x-axis [24]. The radial angle of the arc is clearly found to increase gradually with increasing immersion intervals. This implies a subsequent decrease in the corrosion rate of the material and suggesting that the passivity of the surface film is gradually enhanced with time. The introduction of a new time constant at low frequency region can be associated with a decrease in magnitude of the semi-infinite behavior, due to the interaction between the electrode and electrolyte interface [36] and hence becomes more evident during prolonged immersion. Moreover, the large broad peak of the phase angle on the Bode format (Fig. 2) could be indicative of an interaction of at least two time constants [19,25]. This is due to a

growth of more resistive layer on the alloy surface, affording better corrosion stability for the material with time. According to our earlier works, the passive film grown spontaneously on SS sample [37], as well as that film formed on TA alloy [25,38], was found to consist from an oxide of a double character with two regions, a dense inner layer and a porous outer layer. The former compact layer acts as a barrier against corrosion and the later layer is permeable to the aggressive species in the electrolyte. Substantial evidences are also reported confirming this structure for the surface films grown on TA [13,19] and on SS [22,30,39] substrates after prolonged immersion in simulated body fluid (SBF).

The objective of ac impedance technique is to model the corrosion process in terms of circuit elements in order to enable an accurate analysis for the obtained EIS data, and make conclusions about the mechanism and properties of the corrosion process. Therefore, based on the above facts, Thales software provided with the measuring workstation was used to analyze the obtained spectra in terms of the electronic equivalent circuit (EEC) shown in Fig. 4.
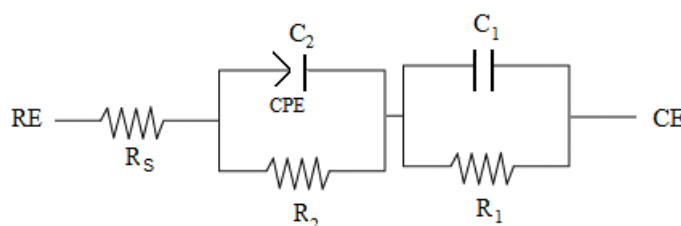
Figure 4. Electrical equivalent circuit model representing impedance spectra with two series time constants used to fit the experimental EIS data for SS and TA samples in the tested physiological solutions.

This types of EEC is commonly proposed to mimic passive film with duplex nature formed on Ti materials [13] and stainless steel alloys [22,39] under simulated physiological environments. The model consists of two circuits in series from R_1C_1 and R_2Q_2 parallel combinations and the two are in series with the solution resistance (R_s) between the alloy surface and the reference electrode. In this way, the two time constants R_1C_1 and R_2Q_2 at the low and medium frequency ranges are the resistance and capacitance of the inner and outer layers, respectively. As a matter of fact, it is worth to note that the dispersion behavior observed at rough electrodes can be described by a constant phase element (CPE) of the form [30,39,40]:

$$Z_{CPE}(\omega i) = 1/Q(i\omega)^{\alpha} \qquad\qquad (1)$$

Depending on the exponent α, the CPE can represent capacitance ($\alpha = 1$, $Q = C$), resistance ($\alpha = 0$, $1/Q = R$), or Warburg impedance ($\alpha = 0.5$, $1/Q = W$). For real polished electrodes, the value of α is less than 1, and the lower the value the rougher the electrode surface [41]. α is often denoted as a fit parameter, i is the imaginary root ($\sqrt{-1}$) and the angular frequency $\omega = 2\pi f$ rad s^{-1}, f being the applied frequency in Hz (s^{-1}). The constant Q in Ω^{-1} s$^{\alpha}$ cm^{-2} accounts for a combination of properties related to both the surface and the electroactive species, where its value will be identical to the total capacitance (C) of the CPE at $\omega = 1$ [25]. Values of the simulated electronic impedance parameters in the two

tested media as a function of the exposure time are then calculated and listed in Tables 1 and 2 with an average error of less than 2%.

Generally, the results reveal that the layer resistances of the passive film R_1 and R_2 are always in the order of $k\Omega$ cm^2. However, for both samples in RS solution the resistance (R_1) of the inner layer is much higher than R_2 of the outer layer at all immersion times. Also, the capacitance C_1 of the inner layer is higher than C_2 of the outer layer (Table 1). Since theoretically, film capacitance (C, in μF cm^{-2}) is inversely proportional to its thickness (d, in cm) according to the relation [25]:

$$1/C = d/\varepsilon_o\varepsilon_r \tag{2}$$

where ε_o is the permittivity of free space (8.854×10^{-14} F cm^{-1}) and ε_r is the relative dielectric constant of the film. Therefore, the above trend for the two materials in RS solution indicates that although the inner layer of the surface film is thinner, it is more passive than its thicker outer layer. Nevertheless, in PBS solution (cf. Table 2) a reverse trend for the layer resistance is obtained, where R_2 becomes larger than R_1, while the capacitance C_1 at all exposure periods remains at higher values than C_2, as in the RS solution. The nature of the prevailing anion in a saline medium has an inductive impact on the passive properties of the two tested biomaterials (SS and TA).

Table 1. Electrochemical impedance parameters as a function of the immersion time in Ringer saline (RS) solution.

(a) For type 316 stainless steel (SS)

Time (t)	R_1 (kΩ cm^2)	C_1 (μF cm^{-2})	R_2 (kΩ cm^2)	C_2 (μF cm^{-2})	α	R_s (Ω cm^2)
10 min	8.4	296.92	2.9	53.62	0.731	7.5
1 h	106.4	243.58	8.2	67.77	0.745	7.7
2 h	154.7	187.87	9.9	62.16	0.769	8.6
4 h	123.7	123.01	2.3	61.99	0.773	8.5
6 h	139.5	112.09	2.4	57.02	0.763	8.4
1 d	188.5	81.84	2.5	42.06	0.734	7.0
3 d	235.1	76.95	1.6	33.74	0.707	5.8
7 d	281.8	62.94	2.7	35.37	0.741	5.0
11 d	320.9	69.82	2.9	35.37	0.752	4.2
14 d	332.2	55.36	3.8	26.89	0.719	5.0

(b) For Ti-6Al-4V alloy (TA)

Time (t)	R_1 (kΩ cm^2)	C_1 (μF cm^{-2})	R_2 (kΩ cm^2)	C_2 (μF cm^{-2})	α	R_s (Ω cm^2)
10 min	41.4	95.46	6.2	12.49	0.731	7.6
1 h	98.5	76.60	4.2	13.84	0.729	8.1
2 h	123.0	78.83	62.7	13.40	0.734	8.2
4 h	136.0	69.97	97.7	13.02	0.731	8.5
6 h	139.6	66.95	112.3	13.23	0.734	8.4
1 d	164.2	64.58	159.8	13.43	0.765	5.7
3 d	364.3	59.04	323.5	10.28	0.771	7.4
7 d	616.2	82.59	586.6	11.98	0.782	5.2
11 d	1169.7	69.50	1078.9	12.38	0.794	5.6
14 d	910.0	43.48	282.0	13.43	0.756	5.7

Table 2. Electrochemical impedance parameters as a function of the immersion time in phosphate buffer saline (PBS) solution.

(a) For type 316 stainless steel (SS)

Time (t)	R_1 (kΩ cm^2)	C_1 (μF cm^{-2})	R_2 (kΩ cm^2)	C_2 (μF cm^{-2})	α	R_s (Ω cm^2)
10 min	2.9	373.76	202.0	26.78	0.774	5.4
1 h	4.0	402.48	235.7	45.78	0.811	7.9
2 h	7.5	453.55	380.1	37.73	0.872	8.0
4 h	8.5	400.36	402.4	30.59	0.883	7.3
6 h	93.8	403.90	2357.2	30.55	0.837	7.2
1 d	116.8	68.30	2532.2	26.70	0.897	8.5
3 d	294.4	47.77	3094.6	22.29	0.872	6.0
7 d	538.9	41.28	3450.5	21.75	0.857	6.7
11 d	528.8	39.11	11101.3	21.79	0.853	6.3
14 d	298.1	43.09	5155.0	24.37	0.823	5.7

(b) For Ti-6Al-4V alloy (TA)

Time (t)	R_1 (kΩ cm^2)	C_1 (μF cm^{-2})	R_2 (kΩ cm^2)	C_2 (μF cm^{-2})	α	R_s (Ω cm^2)
10 min	25.4	183.97	602.0	42.13	0.812	6.6
1 h	47.1	199.79	1211.0	37.48	0.864	6.3
2 h	55.5	203.01	1328.0	36.38	0.878	6.1
4 h	58.5	191.63	1414.8	33.99	0.881	6.6
6 h	99.3	183.37	2600.0	33.63	0.983	8.5
1 d	104.1	142.80	2719.6	22.41	0.884	8.8
3 d	141.5	60.25	4035.4	21.74	0.827	7.9
7 d	182.0	59.65	5344.0	20.64	0.895	6.9
11 d	368.3	44.47	11499.0	22.63	0.871	5.5
14 d	258.5	46.45	762.0	21.74	0.872	4.5
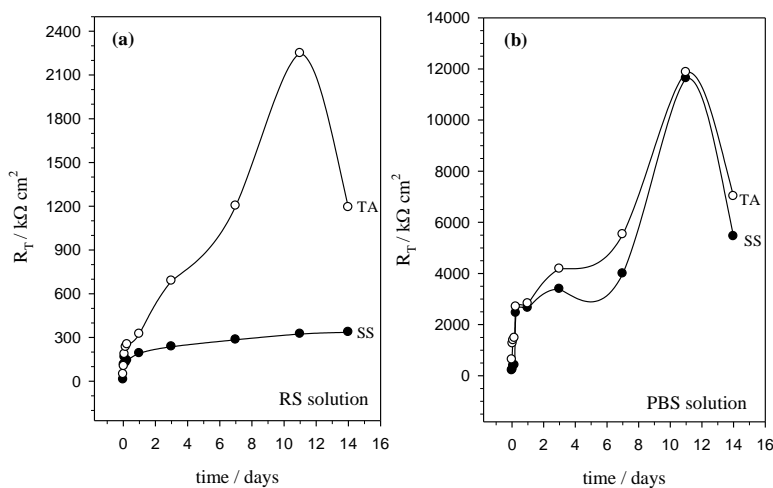
Figure 5. The total film resistance (R_T) for both SS and TA samples in (a) RS solution and (b) PBS solution as a function of time in days.

Thus, from the corrosion point of view incorporation of PO_4^{3-} anion prevailing in the PBS electrolyte into the outermost layer of the passive film significantly reduces its porosity and suppresses metal dissolution. This would lead to an increase in R_2 value of the outermost layer in comparison to R_1 value of the innermost layer, as found experimentally. During the first eleventh days, Fig. 5 demonstrates that for each sample in either media, there is a continuous increase in the total resistance ($R_T = R_1 + R_2$) of the passive film with increasing exposure time. Since from Stern–Geary equation [42], the corrosion current density: $j_{corr} = B/R_p$, where R_p is represented by R_T of the passive layers [39] and B is a constant determined by Tafel slope analyses. It follows then that the higher R_T value, the lower is the corrosion rate and, subsequently the lower will be the ion release from the sample. After the day eleventh, R_T decreases in all cases except for the case of SS sample in RS solution, which experiences insignificant increase in its R_T value as compared with the significant increase for the other three cases. On the other hand, the results clearly reveal that in RS solution after the end of the second day R_T for TA resumes a relatively fast increase in its value compared to its meager increase for SS.
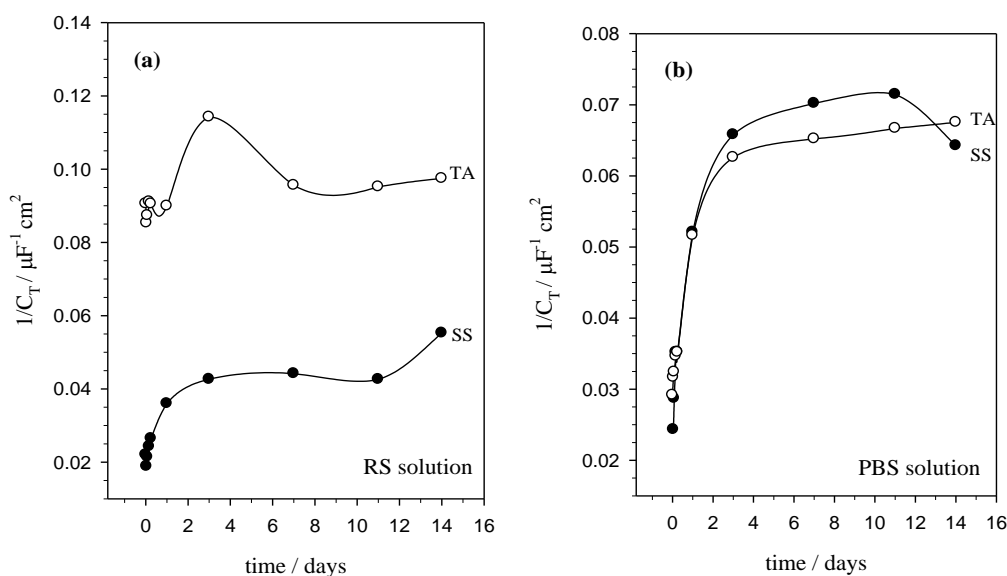
Figure 6. The relative film thickness ($1/C_T$) for both SS and TA samples in (a) RS solution and (b) PBS solution as a function of time in days.

Furthermore, in PBS solution the passive film formed on TA exhibits a somewhat lower R_T value relative to that for SS up to the end of the second day. But, as the immersion time is more prolonged the two samples elicit generally similar trend with a little improvement in favor of TA sample. Eventually, at the end of the day eleventh R_T values for both materials become comparable to each other and resume a fast decrease with a larger rate for SS than for TA alloy. Accordingly, it can be expected that in terms of the corrosion stability and passive properties both tested biomaterials have a quite close performance in PBS solution. A collateral reason for this trend can be attributed primarily to the tendency of the oxide porous layer for hydration; thereby phosphate anions forming PBS solution may be easily incorporated into the pores and further precipitated leading to corrosion or self-healing.

The behavior of the total relative film thickness ($1/C_T = 1/C_1 + 1/C_2$) shown in Fig. 6 further confirms that although the surface film formed on TA in RS fluid is thicker than the one formed in PBS, yet it is less protective. The reverse trend between R_T and $1/C_T$ for TA biomaterial suggests that RS solution can stimulate the oxidation rate of TA more than PBS does. This would lead to the formation of a thicker passive film with more porous nature in RS as compared to the thinner but more compact and densified oxide film formed on TA sample in PBS fluid. On the other hand, for SS the behavior of the relative film thickness ($1/C_T$) is mirrored completely by the trend of its total resistance (R_T). This indicates that thicker film formed on SS substrate in PBS affords better protection due to sealing of its pores by precipitation of phosphate ions abound in the environment. In this respect, other authors [30] have revealed the protective effect of phosphate on the 316L SS material in PBS solution which can change film growth kinetics and improve its passive behavior by increasing the charge transfer resistance and decreasing the capacitance. Furthermore, it can be observed that in RS solution the total relative thickness ($1/C_T$) of the film grown on SS substrate is relatively much smaller than that formed on TA, suggesting that RS has more corrosive action on SS than on TA. The behaviour is likely attributed to the detrimental aggressive attack of Cl⁻ ions on stainless steel [24,30], and subsequently in RS environment the passive film grown on TA material at any given time interval would be thicker and more protective than that grown on SS substrate.

3.3. Polarization curves analyses
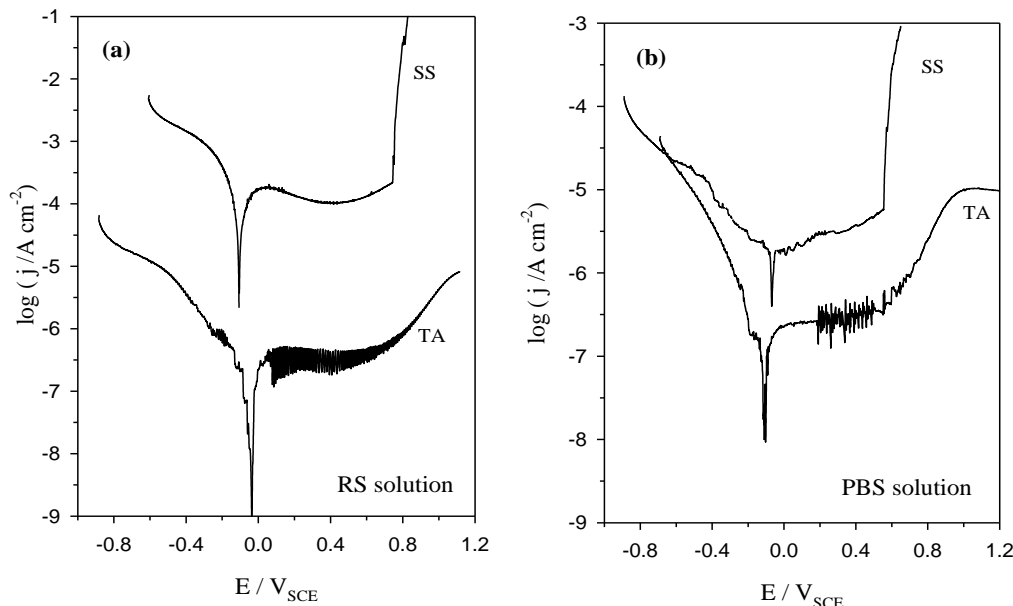
Figure 7. Cathodic and anodic potentiodynamic scans for both 316L stainless steel (SS) and Ti-6Al-4V alloy (TA) after 14 d immersion in (a) Ringer saline (RS) solution and (b) phosphate buffer saline (PBS) solution.

Fig. 7 shows typical log *j-E* cathodic and anodic potentiodynamic scans for SS and TA samples after 14 d immersion in naturally aerated quiescent RS and PBS solutions. As can be seen, the polarization curves behave in a very similar manner. On increasing the potential, each alloy reaches its

respective passive current density (j_p) depending on the chemistry of the tested medium. The observed partial stabilization of j_p in both cases implies that a protective anodic oxide film is formed on the sample surface. The small oscillations of current density seen in the passive region of TA sample in either physiological solution RS or PBS may be related to the consecutive formation and repassivation of micro-sized pits, commonly called metastable pits [43,44]. This is commensurate with some microscopic breakdown events observed far below the pitting potential (E_{pit}). E_{pit} is a critical potential value (breakdown potential) under which the aggressive species in solution, generally chloride ion could penetrate the surface film [45]. Pitting corrosion certainly causes metal failure by creation of small holes in a surface that is normally passive. When E_{pit} is exceeded, the measured current density starts to rise continuously with increasing potential because pits propagate by anodic dissolution of the metal. Hence, E_{pit} value describes the transition potential above which pits can propagate in a stable growth mode [43-47]. Values for the average corrosion potential (E_{corr}), corrosion current density j_{corr}, E_{pit} and j_p were all estimated and listed in Table 3.

Table 3. Electrochemical corrosion parameters for type 316L stainless steel (SS) and Ti-6Al-4V alloy (TA) samples after 14 days immersion in Ringer saline (RS) and phosphate buffer saline (PBS) solutions.

Solution	E_{corr} (V_{SCE})	j_{corr} (A cm^{-2})	E_{pit} (V_{SCE})	j_P (A cm^{-2})	ΔE^a (V)
RS For SS sample	-0.107	1.12×10^{-4}	0.668	1.09×10^{-4}	0.775
For TA sample	-0.052	1.37×10^{-7}	0.776	4.10×10^{-7}	0.828
PBS For SS sample	-0.068	1.55×10^{-6}	0.508	3.00×10^{-6}	0.576
For TA sample	-0.112	6.40×10^{-8}	0.533	2.53×10^{-7}	0.645

[a]ΔE (V) = E_{pit} - E_{corr}

In addition, the difference ΔE between the corrosion potential and the pitting potential (i.e. the transition potential) in the anodic region is given in the last column of this table. In all cases, the corrosion potentials are somewhat more negative than those obtained from the OCP measurements. This is because the polarization scans were started at a more cathodic potential relative to the OCP, so that the passive film at the surface was at least partially removed due to the highly reducing initial potential [19,44].

The results of Table 3 disclose that TA sample after 14 days immersion in RS solution has much lower j_{corr} and j_p values of 0.137 and 0.410 μA cm^{-2} in comparison to those for SS sample (0.012 and 0.109 mA cm^{-2}, respectively). This means that TA has higher improved corrosion resistance than SS in Ringer's fluid as manifested also by the higher ΔE value for TA. The results are in good

agreement with the above analyses for OCP and EIS data. On the other hand, in PBS solution there is a relatively small improvement in the corrosion stability and passive performance of TA sample as compared to the large enhancement in the corrosion resistance and passive behaviour of SS sample in this environment. As for TA sample the two current densities j_{corr} and j_p in PBS solution become almost half their values in RS. While for SS sample both parameters are decreased by two orders of magnitude in PBS fluid than in RS. However, as suggested by Burstein et al. [43] a significant fraction of the passive current density of Ti in physiological solutions may be due to the microscopic breakdown process, which occurs at quite modest electrode potentials, well below the pitting potential. By considering the difference ΔE between E_{corr} and E_{pit} values, it is obvious that for SS and TA samples although the spontaneous corrosion occurs more easily in RS than in PBS fluid, the pitting corrosion occurs more readily in PBS solution [28]. Moreover, the results of Fig. 7 and values of ΔE indicate that PBS solution can stimulate metastable pit propagation events on the specimen surface and increases its pitting susceptibility more than RS solution does. These events constitute a significant fraction of the passive corrosion rate of TA biomaterial, albeit they are rare events for SS sample compared with TA. As such, the propensity of the two samples, especially TA, for growing metastable pits is of fundamental importance to the mechanism of their passivity in physiological systems.

3.4. Surface analyses
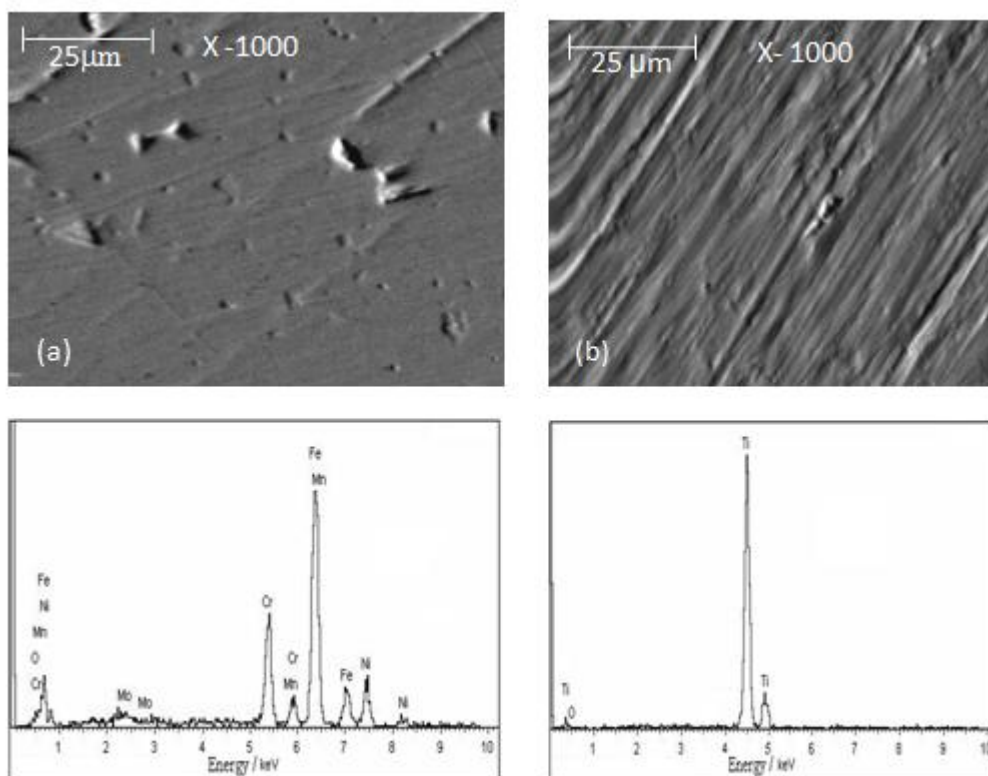
Figure 8. SEM-EDX surface analysis of: (a) 316L stainless steel (SS) and (b) Ti-6Al-4V alloy (TA) after 11 d immersion in Ringer saline (RS) solution.
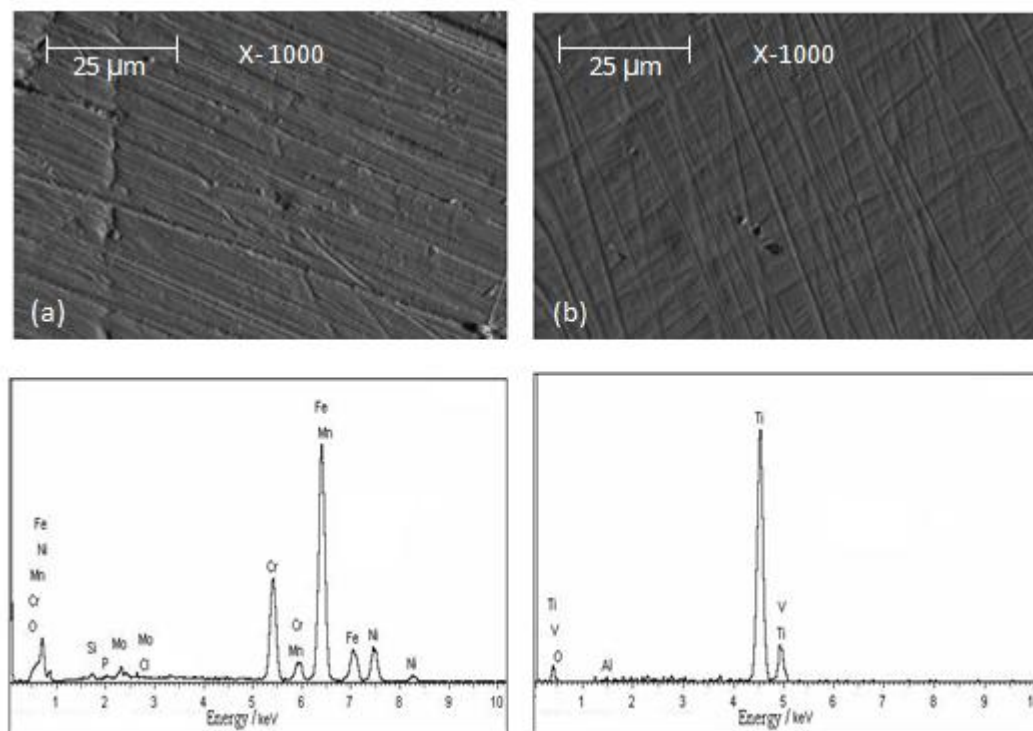
Figure 9. SEM-EDX surface analysis of: (a) 316L stainless steel (SS) and (b) Ti-6Al-4V alloy (TA) after 11 d immersion in phosphate buffer saline (PBS) solution.

The surface morphologies and EDX spectra shown in Figs. 8 and 9 in the two tested physiological solutions for both SS and TA samples are generally consistent with the above electrochemical behavior. For specimens immersed eleven days in RS solution (Fig. 8), the image reveals a lot of small pits over the entire surface of SS sample, but few pits can be observed on the surface of TA biomaterial. The EDX spectrum for SS exhibit various peaks pertinent to the elements composing the sample, namely, Fe, Cr, Ni, Mn and Mo, beside a peak for oxygen, suggesting that the surface passive film is formed by a mixture of oxides [48] representing those elements. On the other hand, the EDX spectrum of TA sample exhibits well defined peaks corresponding to Ti as well as a peak for oxygen, whereas the other metals in the alloy do not appear. These results denote to the formation of a single Ti oxide film on TA substrate during immersion that possesses higher resistance to the pitting action of Cl$^-$ ions constituting Ringer's biofluid. Regarding the two specimens immersed eleven days in PBS fluid, the corresponding SEM images shown in Fig. 9 reveal nearly comparable surface morphologies to each other, as well as a notable improvement in their microstructures compared to those observed in Fig. 8. Furthermore, it is worth to indicate that the EDX spectrum of SS sample in PBS solution (Fig. 9a) discloses the presence of phosphorus (P) peak, likely coming from contamination of the surface oxide film by PO_4^{3-} ions abound in the used physiological solution. The contaminated phosphate endows a better enhanced passivity and corrosion resistance for the growing oxide film compared to the one formed in RS solution (Fig. 8a). Additionally, for TA sample (Fig. 9b) the EDX spectrum reveals the presence of Al and V peaks along with the main two peaks for Ti and O. For this case, it seems that the growing passive oxide film which is modified by Al and V has stronger

protective and insulating properties than the non modified surface film. This would decrease the bio-corrosion effect of the implant and enhance its stability in PBS, thereby reducing the possibility of introducing foreign metallic ions into a stable physiological system.

4. CONCLUSIONS

The surface integrity of two medical alloys, namely 316L stainless steel (SS) and Ti-6Al-4V alloy (TA) were compared based on their electrochemical behavior in Ringer saline (RS) and phosphate buffer saline (PBS) physiological solutions. Such alloys can be spontaneously passivated with time as revealed by the OCP measurements. On the other hand, EIS results indicate a high capacitive behavior typical of passive materials due to the growth of very resistive oxide film on the substrate. The formed passive oxide has a bi-layered character and can be satisfactorily modeled by two time constants electronic circuit. In all cases, a continuous increase in the oxide film resistance is observed during the first 11 days which decreases afterwards. Accordingly, the reduction observed in the impedance value indicates a decrease in the surface stability of the materials. The results indicated that in RS solution the corrosion performance of the SS is exceptionally inferior due to the deleterious aggressive attack of Cl^- ions on the substrate. This affords a growth of thin and less protective passive film. On the other hand, in PBS medium, incorporation of the prevailing PO_4^{3-} ions into the growing film increases greatly the film thickness and its total resistance. As for TA, both OCP and EIS data indicated that although RS fluid sustains the growth of a thick passive oxide layer, PBS medium plays a role in modifying the interface behavior of TA and enhancing the growth of thinner film with better improved protective ability.

Polarization analyses revealed that TA in PBS solution has very low (order of nA cm^{-1}) corrosion current (j_{corr}) and passive current (j_p) densities, which are almost half their values in RS. This indicates higher corrosion resistance for TA sample in PBS medium. On the other hand, SS in RS solution has higher j_{corr} and j_p values (as fractions from mA cm^{-2}). However, in PBS solution these values become 100 times lower (order of μA cm^{-1}); suggesting a more developed surface film passivity leading to a significant reduction in the corrosion susceptibility of SS. Our SEM and EDX analyses confirmed that the behavior of the two biomaterials becomes closely similar in PBS environment. Further studies are needed to evaluate the effect of adding protein to the physiological solution on the overall integrity of the metal alloy biomaterials.

References

1. G. Manivasagam, D. Dhinasekaran, A. Rajamanickam, *Recent patents on Corrs. Sci.*, 2 (2010) 40-54.

2. M . Metikoš-Huković, Z. Pilić, R. Babić, D .Omanović, *Acta Biomaterialia,* 2 (2006) 693 700.
3. S. Virtanen, I. Milošov, E.Gomez- barrenas R. Trebše, J.Salo, Y.T.Konttinen, *Acta Biomater.,* 4 (2008) 468-476.
4. P.I. Branemark, B. Hansson, R. Adell, U. Breune, J. Lindstron, O. Halen, A. Ohman, Osseointegrated implants in the treatment of the edentulous law, Almquist Swikssell, Stockolm, 1997.
5. G. Giavaresi, L. Ambrosio, G. A. Battiston, U. Casellato, R. Gerbasi, M. Finia, et al., Bio*materials*, 25 (2004) 5583-5591.
6. L.Thair, T. Ismaeel, B. Ahmed, A.K. Swadi, *Surf. Eng.,* 27(2011) 11-18.
7. M. Navarro, A. Michiardi, O. Castaňo, J.A. Panell, *J. The Royal Soc. Interface,* 5 (2008) 1137-1158.
8. S.G. Steinemann, Corrosion of surgical implants–*in vivo* and *in vitro* tests, in: G.D. Winter, J.L. Leray, K. de Goot (Editors), Evaluation of biomaterials, advances in biomaterials, Vol I. Chichester, Wiley, 1980, p. 1-34.
9. S. Karimi, T. Nickchi, A.M. Afantazi, *Appl. Surf. Sci.*, 258 (2012) 6087-6096.
10. S. Mischler, A. Igual Muñoz, *Wear*, 297 (2013) 1081-1094.
11. J. Cahoon, H.Paxton, *J. Biomed. Mater. Res.,* 2 (2004) 1-22.
12. Y. Okazaki, E. Gotoh, *Biomaterials*, 26 (2005) 11-21.
13. S.Tamilselvi, V. Raman, N. Rajendran, *Electrochim. Acta*, 52 (2006) 839-846.
14. N.T.C. Oliveira, A.C. Guastaldi, *Acta biomater.,* 5 (2009) 399-405.
15. M. Pourbaix, Atlas of electrochemical equilibria in aqueous solutions, 2nd ed., NACE International, Houston TX, 1974.
16. F. Hua, K. Mon, P. Pasupathi, G. Gordon, D. Shoesmith, *Corrosion*, 61 (2005) 987-1003.
17. I. Milošev, M. Metikoš-Hukovic, H.-H. Strehblow, *Biomaterials*, 21 (2000) 2103-2113.
18. M. Long, H.J. Rack, *Biomaterials*, 19 (1998) 1621-1639.
19. S. Luiz de Assis, S. Wolynec, I. Costa, *Electrochim. Acta*, 51 (2006) 1815-1819.
20. Y. Khelfaoui, M. Kerkar, A. Bali, F. Dalard, *Surf. Coat. Tech.,* 200 (2006) 4523-4529.
21. K. Yaya, Y. Khelfaoui, B. Malki, M. Kerkar, *corros. Sci.,* 53 (2011) 3309-3314.
22. R. A. Antunes, M.C. L. de oliveira and I. Costa, *Mater. Corros.*, 63 (2012) 586-592.
23. J.A. Disegi, L. Eschbach, *Injury, Int. Care Injured*, 31 (2000) S-D2-6.
24. F. El-Taib Heakal, A.A. Ghoneim, A.M. Fekry, *J. Appl. Electrochem.*, 37 (2007) 405-413.
25. F. El-Taib Heakal, A.A. Ghoneim, A.S. Mogoda, Kh.A. Awad, *Corros. Sci.*, 53 (2011) 2728-2737.
26. N.T.C. Oliveira, A.C. Guastaldi, *Corros. Sci,* 50 (2008) 938-945.
27. N.T.C. Oliveira,, E.A. Ferreira, L.T. Duarte, S.R. Biaggio, R.C. Rocha-Filho, N. Bocchi, *Electrochim. Acta*, 51 (2006) 2068-2075.
28. N. Maruyama, D. Mori, S. Hiromoto, K. Kanazawa, M. Nakamura, *Corros. Sci,* 53 (2011) 2222-2227.
29. Metals test Methods and Analytical Procedures, Annual Book of ASTM Standards, 03-02, section 3 Philadelphia, USA, 1999, pp. 48-58.
30. C. Valero Vidal, A. Igual Muñoz, *Corros. Sci.*, 50 (2008) 1954-1961.
31. I. Gurappa, *Mater. Character.*, 49 (2002) 73-79.
32. U.R. Evans. The Corrosion and oxidation of metals: Scientific principles and practical applications. London: Edward Arnold Ltd; 1960. p 898.
33. F. El-Taib Heakal, A.M. Fekry, A.A. Ghoneim, *Corros. Sci.*, 50 (2008) 1618-1626.
34. L.L. Shreir, Corrosion, Metal/Environment Reactions, vol I, New-nes-Butterworths, London, 1976, pp 1-22.
35. F. El-Taib Heakal, S. Haruyama, *Corros. Sci.*, 20 (1980) 887-898.
36. S. Tamilselvi, V. Raman, N. Rajendran, *J. Appl. Electrochem.*, 40 (2010) 285-293.
37. F. El-Taib Heakal, M.A. Ameer, A.M. El-Aziz, A.M. Fekry, *Mat-wiss U. Werkstofftech*, 35 (2004) 407-412.

38. F. El-Taib Heakal, Kh.A. Awad, *Int. J. Electrochem. Sci.,* 6 (2011) 6483-6502.
39. G. Rondelli, P. Torricelli, M. Giardino, *Biomaterials,* 26 (2005) 739-744.
40. U. Rammelt, G. Reinhard, *Electrchim. Acta*, 35 (1990) 1045-1049.
41. M. Leibig, T.C. Halsey, *Electrochim. Acta,* 38 (1993) 1985-1988.
42. M. Stern, A. Geary, *J. Electrochem. Soc.,* 104 (1957) 56-63.
43. G.T. Burstein, C. Liu, R.M. Souto, *Biomaterials*, 26 (2005) 245-256.
44. W.Y. Guo, J. Sun, J.S. Wu, *Mater. Chem. Phys.*, 113 (2009) 816-820.
45. Y. Yi, P. Cho, A. Al Zaabi, Y. Addad, C. Jang, *Corros. Sci.*, 74 (2013) 92-97.
46. G.T. Burstein, C. Liu, *Corros. Sci.*, 49 (2007) 4296-4306.
47. G.T. Burstein, C. Liu, R.M. Souto, S.P. Vines, *Corros. Eng. Sci. Technol.*, 39 (2004) 25-30.
48. M.F. López, A. Gutiérrez, J.A. Jiménez, *Surf. Sci.*, 482-485 (2001) 300-305.